Purdue University
Purdue e-Pubs

School of Aeronautics and Astronautics Faculty Publications

School of Aeronautics and Astronautics

2010

Experimental Determination of the Key Heat Transfer Mechanisms in Pharmaceutical Freeze Drying

Arnab Ganguly
Purdue University

Steven L. Nail

Alina A. Alexeenko
Purdue University - Main Campus, alexeenk@purdue.edu

Follow this and additional works at: http://docs.lib.purdue.edu/aaepubs

Part of the Engineering Commons

Experimental Determination of the Key Heat Transfer Mechanisms in Pharmaceutical Freeze Drying

Arnab Ganguly[1]
School of Aeronautics and Astronautics, Purdue University, West Lafayette, IN 47907, USA

Steven L. Nail [2]
Baxter Pharmaceutical Solutions LLC, Bloomington, IN 47403, USA

Alina A. Alexeenko[3]
School of Aeronautics and Astronautics, Purdue University, West Lafayette, IN 47907, USA

Freeze-drying is often used in manufacture of pharmaceuticals to remove a solvent in such a way that the sensitive molecular structure of the active substance of a drug is least disturbed, and to provide a sterile powder that can be quickly and completely rehydrated. In this work heat transfer rates in a laboratory-scale freeze-dryer have been measured to investigate the contribution of different heat transfer modes. Pure water was partially dried under low-pressure conditions and sublimation rates were determined gravimetrically. The heat transfer rates were observed to be independent of the separation distance between a product vial and a dryer shelf and linearly dependent on the pressure in the free molecular limit. However, under higher pressures the heat transfer rates were independent of pressure and inversely proportional to the separation distance. Previous heat transfer studies in conventional freeze-drying cycles have attributed a dominant portion of the total heat transfer to radiation, the rest to conduction, whereas the convection has been found insignificant. While the measurements revealed the significance of the radiative and gas conduction components, the convective component was found to be comparable to the gas conduction contribution at pressures greater than 100mTorr. The current investigation suggests that the convective component of the heat transfer cannot be ignored at typical laboratory-scale freeze-drying conditions.

Nomenclature

q	=	Heat flux, Wm^{-2}
α	=	Thermal accommodation coefficient
Λ_0	=	*F*ree molecular heat conductivity at 0°C, $\text{Wm}^{-2}\text{K}^{-1}\text{Pa}^{-1}$
P	=	Pressure, Pa
T_h	=	Shelf temperature, K
T_c	=	Vial temperature, K
T_{ref}	=	Reference temperature, K

---

[1] Graduate Student, School of Aeronautics and Astronautics, Purdue University, West Lafayette, IN, 47907, student member AIAA

[2] Sr. Baxter Research Scientist, Baxter Pharmaceutical Solutions LLC, Bloomington, IN, 47403

[3] Assistant Professor, School of Aeronautics and Astronautics, Purdue University, West Lafayette, IN, 47907, AIAA Senior Member, Email: alexeenk@purdue.edu

K	=	Heat conductivity of the gas, $Wm^{-1}K^{-1}$
l	=	Separation between the shelf and Vial, m
σ	=	Stefan Boltzmann constant, $Wm^{-2}K^{-4}$
ε	=	Emissivity
R	=	Specific gas constant, $JK^{-1}mol^{-1}$
k	=	Boltzmann constant, $m^2Kg.s^{-2}K^{-1}$

I. Introduction

Pharmaceutical and biopharmaceutical products are often prepared initially as aqueous solutions. Removal of the solvent improves their stability. It is, however, important to remove the solvent in such a way that the sensitive molecular structure of the product is preserved. This is usually done by freeze-drying which consists of a) an initial freezing stage followed by b) sublimation of ice during the primary drying stage and c) secondary drying stage can be used after primary drying to remove the remaining moisture at an accelerated rate. Primary drying is usually the most time and energy consuming stage of freeze-drying and the study of heat transfer mechanisms during this stage has the largest potential for improving the overall freeze-drying process efficiency.

A schematic of a typical pharmaceutical freeze-dryer is shown in Figure 1. The freeze-drying chamber contains the product in vials that are usually in direct contact with shelves, the temperature of which is controlled by a passage of heat-transfer fluid. The rate of water vapor sublimation is dependent on both the shelf temperature and the chamber pressure. The pressure is usually controlled by introducing a non-condensable gas such as nitrogen into the chamber with vials. The water vapor and non-condensable gas flows from the chamber to the condenser reservoir driven by pressure and concentration gradients. In most pharmaceutical freeze-dryers, there is a duct connecting the chamber to condenser reservoir.

The condenser reservoir contains an arrangement of coils or plates that are maintained at a low temperature. Typically the temperature of the condenser coils ranges from -90 C to -50 C. The condenser reservoir is connected to a vacuum pump for removal of non-condensable gases. The typical range of pressures encountered in the freeze-drying systems is from 10 to 500 mtorr.
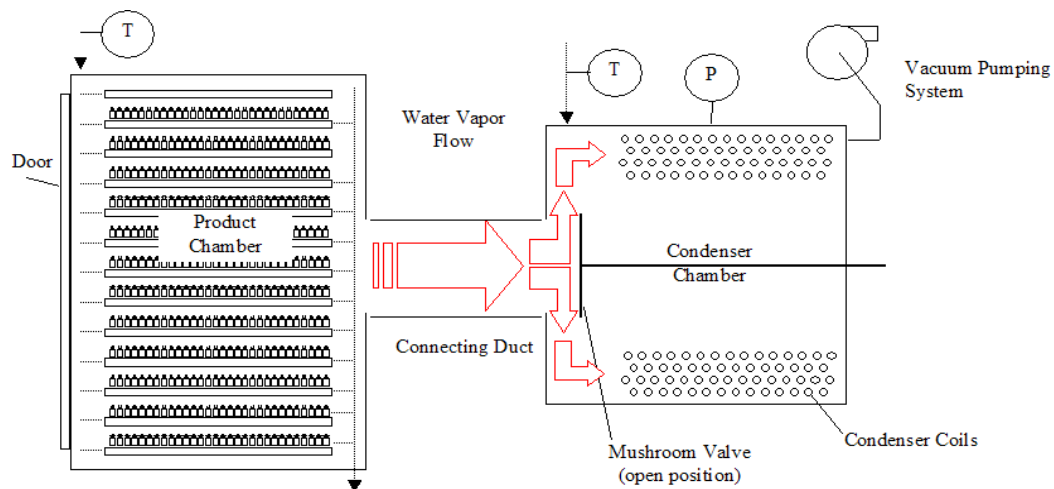

Figure 1: Schematic of a typical pharmaceutical freeze-dryer.

Most of the research in pharmaceutical freeze-drying has dealt with processes and equipment – both laboratory and industrial, in which the product is dried in vials placed directly on heated shelves. Major aspects of the associated heat transfer processes have been discussed by Steven L. Nail in Ref.[1]. In particular, the significance of

2

American Institute of Aeronautics and Astronautics

the lack of intimate contact between the shelf and the vials and its effect on the heat transferred to the vial has been pointed out.

The sublimation rate of frozen solutions of water, aqueous Potassium Chloride, aqueous povidone and mannitol were discussed by Michael J Pikal et al [2] as a function of their freezing rate, product temperature, residual air pressure, solute concentration and the product thickness. It was concluded that the water vapor escapes through pores created in the product due to prior sublimation.

A detailed discussion of the calculation of vial heat transfer coefficient and the contribution of each heat transfer mode to the total heat transferred in a freeze-drying cycle was made by Pikal and co-workers in Ref. [3]. It was shown that the rate of removal of water vapor from the vials during the primary drying is governed by three resistances: resistance of the dried-product layer, resistance of the vial, and the resistance of the chamber to condenser pathway. Further, in Ref. [4] Pikal investigated the effect of chamber pressure and shelf temperature on the drying time and product temperature. The experiments were used to determine the heat and mass transfer coefficients and the associated resistance to heat transfer during primary drying.

Rambhatla et al in Ref [5] estimated the differences in heat and mass transfer due to design characteristics of freeze-dryers. Tests performed were used to evaluate non-uniformity in shelf surface temperatures, resistance of piping, refrigeration system, and condenser. It was found that a front vial in the laboratory dryer received 1.8 times more heat than a front vial in a manufacturing freeze dryer operating at a shelf temperature of –25°C at a chamber pressure of 150 mTorr during primary drying. This is largely because the chamber door in laboratory freeze dryers are usually constructed of Plexiglass, and the door of production equipment is nearly always stainless steel. There is a significant difference in thermal emissivity of the two materials. Wei et al in Ref [6] determined the spatial distribution of the local shelf heat transfer coefficient Ks, by mapping the transient temperature response of the shelf surface along the serpentine internal channels of the shelf. It was found that the values of Ks close to the inlet were significantly higher than those at other locations of the shelf channel, the pattern being attributed to the flow pattern of heat transfer fluid within the channels.

The effects of loading were investigated by Henning in Ref. [7] and by Patel et al in Ref. [8] systematically studied the effects of variation in product load on freeze drying behavior in laboratory, pilot and clinical scale freeze-dryers. It was found that there was no systematic variation in the residual moisture content and vapor composition as load decreased. While Pikal et al in Ref [9] developed nonsteady theoretical models of the freeze-drying process to obtain information such as moisture distribution and glass transition temperature, Tg, within a vial during processing, Sheehan P in Ref. [10] developed a spatially multidimensional model that was solved to describe the dynamic behavior of the primary and secondary drying stages. It was found that heat input control that runs the process close to the melting and scorch temperature constraints yielded (i) faster drying times, and (ii) more uniform distributions of temperature.

A brief analysis of the suspended vial configuration was done by S. Rambhatla et al in 2003 [11] where it was concluded that there was no observed change in the sublimation rate for varying pressures, establishing that radiation was the primary source of heat transfer for such an arrangement.

The goal of this study is to examine systematically, the role of conduction, convection and radiation during primary drying in the absence of contact between the vial and the shelf. The investigation of heat transfer for configurations where there is no direct contact between the vials and the freeze-dryer shelves is motivated in part by the interest in freeze-drying injectable pharmaceutical products in pre-filled syringes with no contact between the product container and the shelf. There has not been a systematic heat transfer analysis for such a configuration. In an attempt at understanding the role played by each heat transfer modes in the absence of contact between the product and the shelf, we present results of measurements of the position-dependence of sublimation rates of ice from suspended vials in a laboratory-scale dryer. Furthermore, the contribution from radiation, conduction and convection in primary drying has been quantified.

The remainder of the paper is organized as follows. Section II gives a brief overview of freeze-drying and the associated heat transfer mechanisms, analytical solutions for heat transfer through conduction, radiation and convection between the shelf and the vial. Section III describes the experimental setup and the procedure adopted. Section IV discusses the results of studies of the position dependence of heat transfer and the individual heat transfer contributions.

II. Theory

Currently, most industrial pharmaceutical freeze-drying processes use a freeze-drying chamber that contains the product in vials which are in direct contact with heated shelves. For cycles in which vials are loaded on the shelf, a primary source of heat transfer to the vials is through the stainless steel shelf on which the vial is placed. However for suspended vials, direct contact between the vial and the shelf is eliminated and the walls of the freeze-dryer, the shelf above the vials and the front glass door would be expected to play a larger role in the heat exchange with the vials. The front glass door plays a significant role in contributing to the radiation, resulting in position-dependent drying rates in the vials distributed over the shelf. The modes of heat exchange are heat conduction through the gas between the vial and the surroundings, thermal radiation from the door, shelves and the walls and heat conduction and radiation through the gas that lies between the shelf and the vial bottom. Thus, the heat transfer components comprise the heat conduction through the gas q_{gas}, the radiative heat transfer q_{rad}, the convective component q_{conv} and for the vials placed on the shelf, the direct contact conduction component $q_{contact}$. The role of convection in pharmaceutical freeze drying has been the subject of speculation, and there are no rigorous studies of convection in these systems. The prevailing opinion, however, is that operating pressures in freeze drying are too low for convection to be significant.

A. Heat Conduction between the Vial and the Shelf

Vapor flow that takes place between the shelf and the vial bottom can shift between three different regimes. The regimes are distinguished by referring to the Knudsen number of the flow in the region. The Knudsen number is the ratio of the mean free path of molecules to the width of the gas layer separating the vial bottom and the shelf surface. The different regimes are the continuum regime, temperature-jump regime and the free molecular regime. The different modes of heat transfer are illustrated in Figure 2.

Free molecular flow occurs when the mean free path is about 10 times the gap between the vial and the shelf [12]. The heat flux (q_f) between the surface of the shelf and the vial may be approximated as a 1D heat transfer problem between parallel plates for small separation distances. The often-used approximation based on elementary kinetic theory for the 1D heat flux is given by[13]

$$q_{fm} = \alpha \Lambda_o P \sqrt{\frac{T_{ref}}{T_c}} (T_h - T_c)$$

(1)

Here P represents the ambient pressure in the chamber. T_h and T_c represent the shelf temperature and the vial bottom temperature respectively and α represents the thermal accommodation coefficient, defined by

$$\alpha = \frac{T_r - T_i}{T_s - T_i}$$

(2)

where T_r is the temperature a molecule attains after being reflected from the surface, T_s is the temperature of the surface with which the molecules collide and Ti is the temperature of the incident molecules. Here, for simplicity, we have defined a constant Λ_0 that represents the free molecular heat conductivity at $T_{ref} = 273.15^o$ K, this is given as

American Institute of Aeronautics and Astronautics

$$\Lambda_0 = \frac{1}{2}\frac{\gamma+1}{\gamma-1}\sqrt{\frac{R}{2\pi T_{ref}}} \tag{3}$$

where R is the specific gas constant and γ is the specific heat ratio. A derivation of Eq. (3) can be found in ref. [13].
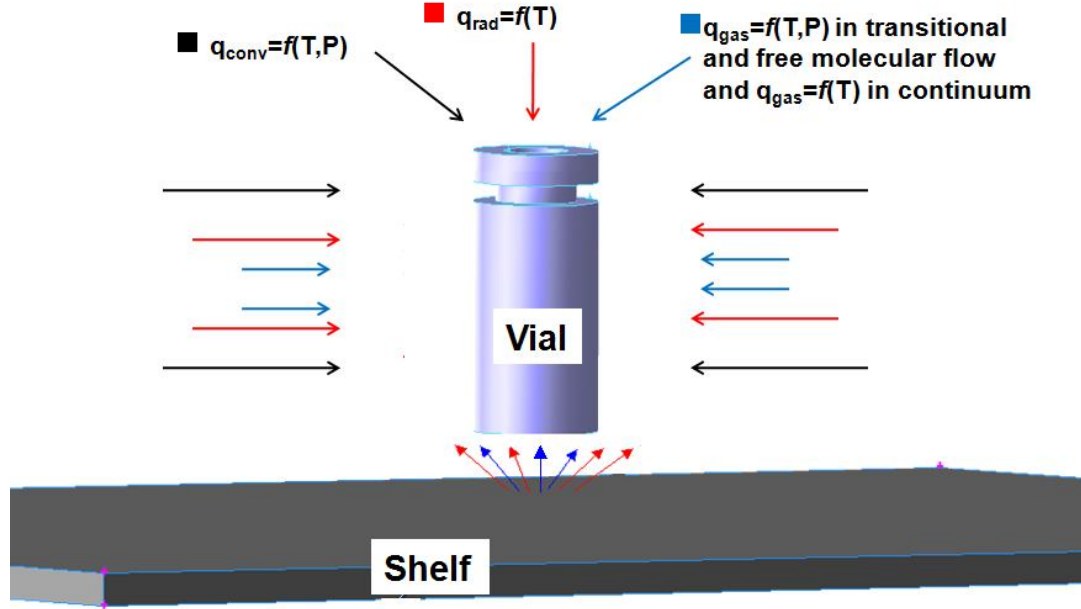

Figure 2. Heat Transfer to a Suspended Vial

The exact analytical solution for free molecular heat transfer between infinite parallel plates is shown below [14]

$$q_{fm} = -\frac{2^{3/2}}{4}\frac{\gamma+1}{\gamma-1}P(\frac{R}{\pi})^{\frac{1}{2}}(T_h^{1/2}-T_c^{1/2}) \tag{4}$$

Here γ represents the ratio of specific heats, P is the ambient pressure in the chamber. T_h and T_c represent the shelf temperature and the vial bottom temperature respectively, R is the specific gas constant and m, the molecular mass. As the Knudsen number decreases (with increase in the separation from the shelf) to about 0.1, the heat flux can be given by the temperature jump equation in the transition regime represented as follows [15].

$$q_{jump} = \frac{T_h - T_c}{\frac{l}{K} + \frac{\sqrt{T_c}}{\alpha\Lambda_0 P\sqrt{T_{ref}}}} \tag{5}$$

Here, l represents the separation between the shelf and the vial surface, K represents the thermal conductivity of the gas, α represents the thermal accommodation coeffcient, Λ_0 represents the free molecular heat conductivity at 0°C and P represents the ambient pressure in the chamber. T_h and T_c represent the shelf temperature and the vial bottom temperature respectively. The Four moment solution for predicting the heat transfer in the temperature jump regime was given by Bird in Ref. [14] and is as represented below.

$$q_{jump} = \frac{[(BT_h + AT_c + \frac{l}{C})^2 - (B^2 - A^2)(T_h^2 - T_c^2)]^{\frac{1}{2}} - (BT_h + AT_c + \frac{l}{C})}{(B^2 - A^2)}$$

(6)

$$A = \frac{1}{2p}(\frac{\pi T_h}{2R})^{\frac{1}{2}} \qquad B = \frac{1}{2p}(\frac{\pi T_c}{2R})^{\frac{1}{2}} \qquad C = \frac{15k^{\frac{3}{2}}}{8(\pi m T_{ref})^{\frac{1}{2}} d_{ref}^{2}}$$

Here A, B and C are as represented above while l is the separation between the parallel plates. Here d_{ref} represents the reference diameter of the water molecule at the reference temperature Tref. A d_{ref} of 5.78Å was used for the calculation at T_{ref}=273.15K [12] and R is the specific gas constant. Finally, as the Knudsen number drops below ~0.01, the heat flux is governed by the continuum regime given by Fourier's heat conduction equation represented by

$$q_{Fourier} = \frac{K}{l}(T_h - T_c)$$

(7)

Figure 3 illustrates the transition from one regime to another and the relative contribution of the gas conduction term in the free molecular, transitional and continuum regimes of flow that may exist in the gap separating the vial and the shelf. The plot is shown for a vial temperature of -40C, a shelf temperature of 25C for a separation of 2mm, filled with water vapor and compares the solution provided by the free molecular solution provided by equations (1) and (4). Also, the heat transfer in the temperature jump regime as given by equations (5) and the four moment solution (6) have been compared. Thus it can be seen that the heat transfer to the vial shifts from being independent of the separation distance in the free molecular regime and linearly dependent on pressure to being independent of pressure and inversely proportional to the separation in the continuum regime. The deviation between the solutions predicted by equations (5) and (6) is due to the four moment solution assuming Maxwell molecules in the gas [14]. Thus, the heat transfer calculations that have been discussed later in this work are based on equations 1, 5 and 7 based on the regime in which the heat transfer takes place.
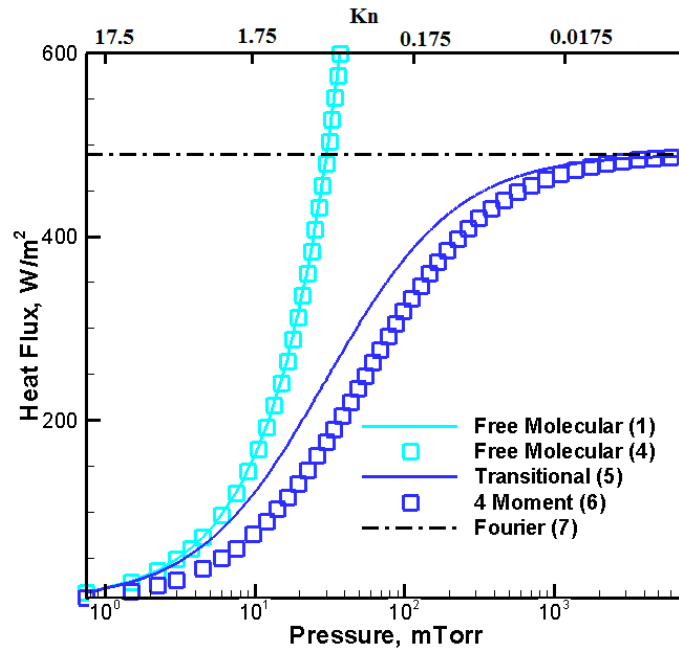

Figure 3. Regime based Heat Flux in the Pressure range 0-1000 Pa for T_h=25C and T_c =-40C

American Institute of Aeronautics and Astronautics

B. Radiative Heat Transfer

The radiative heat transfer component is independent of pressure. It comprises a significant portion of the total heat transfer on account of the large temperature differential (~40K) that exists between the product and the surroundings i.e. the chamber walls, the door etc. The radiative heat flow between two surfaces depends on the difference in the fourth powers of the absolute temperatures of the surfaces, the emissivity of the surface and the area exposed. It is given by the Stefan-Boltzmann relation as

$$q_{rad} = \sigma \varepsilon A (T_2^{\,4} - T_1^4) \tag{8}$$

Where σ is the Stefan Boltzmann constant, ε the emissivity of the surface, A the exposed surface area and T_2 and T_1 the surface temperatures of the two interacting surfaces.

C. Convective Heat Transfer

The convective heat transfer component is pressure dependent and varies as the temperature differential between the surface and the bulk fluid and the area exposed for heat transfer. It is given by the following.

$$q_{conv} = hA(T_s - T_\infty) \tag{9}$$

Here h is the proportionality constant, referred to as the convective heat transfer coefficient, A the exposed area, T_s the temperature of the surface and T_∞ the fluid temperature. The convective heat transfer coefficient is related to a non-dimensional parameter, the Nusselt number Nu by the following relation for flow over a cylinder

$$Nu = \frac{hD}{k} = C\,\mathrm{Re}^m\,\mathrm{Pr}^n \tag{10}$$

Where D is the diameter of the cylinder, k the thermal conductivity of the fluid, C, m and n are constants that depend on the Reynolds number, Re, given by the following relation for a cylinder and Pr the Prandtl number

$$\mathrm{Re} = \frac{\rho V_\infty D}{\mu} \qquad \mathrm{Pr} = \frac{\mu C_p}{k} \tag{11}$$

Here, V_∞ represents the velocity of the fluid and μ the viscosity coefficient. The fluid velocity varies in the freeze-drying chamber depending on the chamber-to-condenser pressure ratio and the position of the vials and the shelves. In general, a complex three-dimensional flow-field develops in the freeze-drying chamber during a primary drying stage when the pressure ratios typically vary from 1.1 to 2. The contribution due to convective heat transfer is difficult to describe analytically and the experimental measurements presented here are one of the first quantitative studies of convective heat transfer rates in freeze-drying. These measurements provide validation data for numerical simulations of vapor flow and heat transfer in freeze-drying.

III. Materials and Methods

A. Materials

To simulate the arrangement of pre-filled syringes in a chamber, an experimental setup was designed that could provide a means of suspending vials at varying separation distances from the shelf. The setup consisted of a stainless structure provided with supports to which a mesh was soldered. The entire structure was made of stainless steel, SS 304. The setup was capable of suspending up to 24 vials. One of the objectives of the design was to minimize the interference to the flowfield in the chamber during the primary drying stage. In order to identify the dominant heat transfer mode in the chamber, it was necessary to analyze the effect of varying separation distances from the shelf, and in effect, identify the effect of gas conduction and conduction through direct contact with the shelves. To vary the separation distance from the shelf, hooks of varying lengths were suspended from the mesh. Aluminum collars were used to firmly grip the vials around the neck. All the experiments were conducted using a 5 ml fill volume of de-ionized water in Kimble 6ml - 20ml throat vials. Figure 4 shows the setup with the vials suspended. A laboratory scale Lyostar II (SP Industries, Stone Ridge, NY) freeze dryer was used for the study.

B. Methods

The experiment consisted of measuring the mass flow rate from the different vials as a function of their separation distance from the shelf. Five vials were suspended, each of them being placed at varying separation distances. One vial was also placed directly on the shelf. An aluminum radiation shield was placed on the inside of the freeze dryer door to reduce the asymmetry in the drying rates caused by the Plexi-glass door. The vials were kept un-stoppered to reduce the uncertainty over the area across which the mass transfer takes place. Thermocouples were positioned to record the temperature variation during the cycle. The setup was placed on insulating thermo-foam pads to reduce heat transfer through the legs of the supporting structure.

Figure 4. Vial Suspension System

1) Setup 1: Suspended Vials with Constant Separation from the Shelves

The two dominant sources of heat transfer to the vials are the front glass door and the shelves. The Plexi-glass door plays an important role on account of the temperature differential between the room temperature and the operating product temperature and the large view factors associated with radiative heat transfer between the door and the vials. This is complimented by the high emissivity of Plexi-glass. The shelves play an important role on account of the large view factor with respect to the vial bottom surface. Thus, studying the effect of radiation and conduction introduces two primary variables, 1) separation from the shelf and 2) the separation from the front glass door.

A drying cycle was designed to quantify the role of the Plexi-glass door. Vials were suspended at increasing distances from the door but maintaining the same separation from the shelf as shown in the schematic in Figure 5. Hooks were used to suspend the vials, placing the bottom surface of the vial at 3.8 inches from the bottom shelf and the top surface at 3.5 inches from the top shelf. Thermocouples were positioned in the vials to obtain real time temperature data during the drying run. The cycle conditions are summarized below.

- Total freezing time: 2 hours

- Shelf set-point temperature during freezing: -50C

- Chamber pressure during drying: 100m torr

- Condenser pressure during drying: 76 m torr

8
American Institute of Aeronautics and Astronautics

- Shelf set-point temperature during drying: -25C

- Drying time: 5 hours
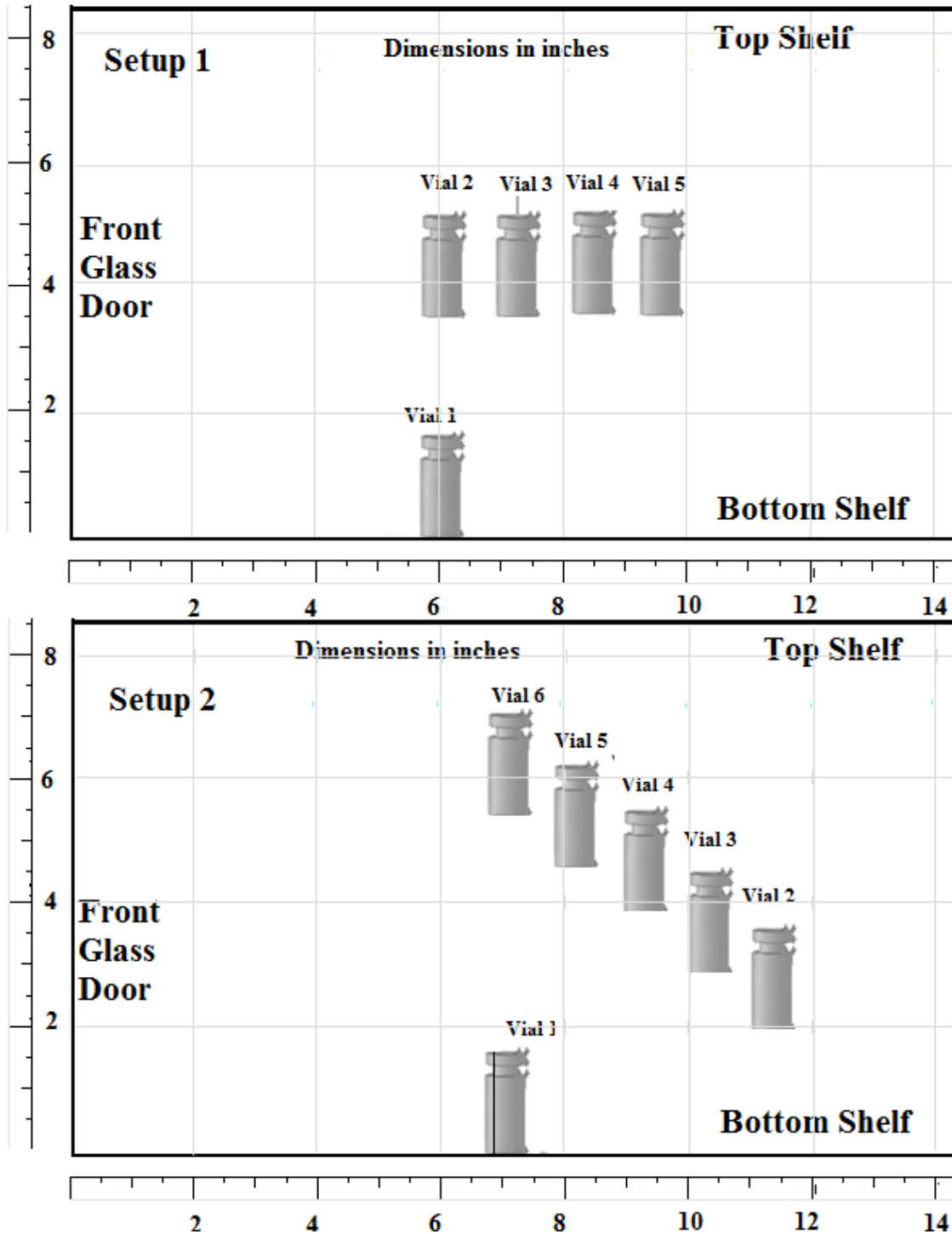
Figure 5. Schematic of the vial positioning in the chamber: (a) Setup 1 and (b) Setup 2

American Institute of Aeronautics and Astronautics

The cycles were allowed to run long enough to dry up to ~20% of the initial fill volumes. This ensured that a quasi steady state was achieved. Subliming a larger quantity of the ice leads to loss of contact between the vial and the ice, introducing uncertainty in the analysis. The sublimation rates were measured gravimetrically.

2) Setup 2: Suspended Vial with varying separation from the shelf and the door

Five vials were suspended, each of them at a different separation from the glass door and the shelf. Apart from this, one vial was also placed directly on the shelf as shown in the Figure 6. The cycle conditions maintained were identical to the ones used for the first setup.

3) Setup 3: Suspended Vials at 1-3mm separation from the shelf

The suspended vials were placed at nominal separation distances of 1, 2, and 3 mm off the shelf. In order to suspend them at such small tolerances, a new apparatus, shown in figure 7 was made. The required separation distances were set using adjusting screws on the bottom of the vial holders. A "bubble level" was used to make sure that the holder was level. A feeler gauge was used to measure the separation distance up to a precision of ± 0.009mm. One holder was placed on each of the three shelves as shown in the Figure 8. The supporting racks were placed six inches back from the front edge of the shelf.
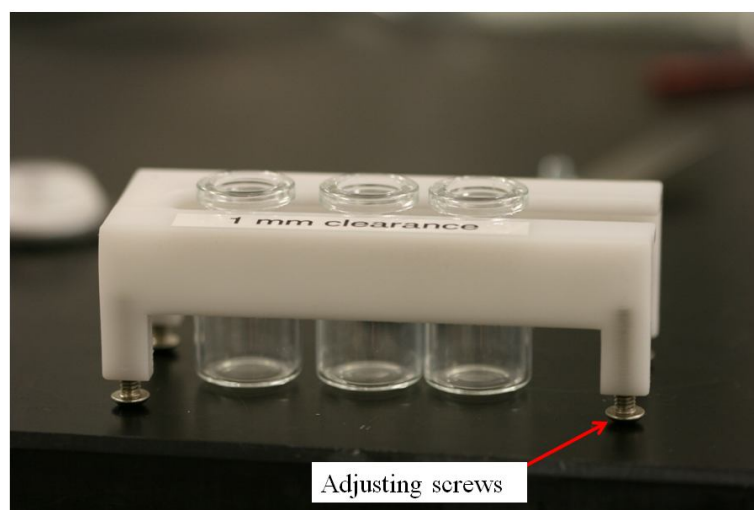

Figure 7. Setup used to suspend vials at 1mm separation from the shelf

One vial was placed directly on the surface of each of the shelves. Thermocouples were mounted to track the temperature of the shelf, the inside of the door, the side wall and the product. In order to establish the pressure dependence of the sublimation rates, the same setup was used for a series of drying runs in which the product was dried under increasing chamber pressures, ranging between 10 and 200 mTorr. A 2.0 ml fill volume of de-ionized water was used. The water was frozen for two hours at -45°C following which, the system was evacuated to the required pressure. The shelf temperature during drying was set to 25° C. The drying period was calculated from the time the shelf reached the set-point temperature. Using this as the cycle starting point, the drying lasted ~1.6 hours. Weight loss data were tabulated and the heat flux calculated using the enthalpy of sublimation of ice, ΔHs. The expression relating the heat flux and the enthalpy of sublimation is given as follows.

$$q = \dot{m}\Delta Hs \qquad (12)$$

10
American Institute of Aeronautics and Astronautics

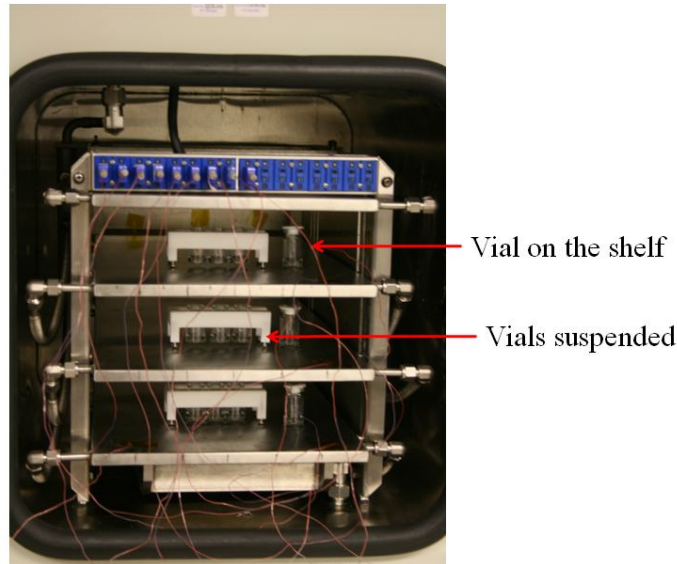where ΔHs is 2803 J/g [1].

Figure 8. Vials placed in the Lyostar II Freeze-dryer before the primary drying cycle with separation distances varying between direct contact-3mm from the shelf

IV. Results

A. Position Dependent Heat Transfer

Flow in the freeze-drying chamber is driven by the heat transfer through the vial walls that leads to an increase in vapor pressure. The chamber pressure is highly uniform and is governed primarily by the vapor pressure inside the vial and the discharge coefficient of the vial orifice. The Figure 9 represents the variation in the sublimation rate for each of the vials used in Setup 1. The sublimation rate decreases as the vial separation from the front door increases even in the presence of the radiation shield. A significant portion of the heat transferred through the Plexiglass door is eliminated due to the presence of the radiation shield. While vial 1, placed on the shelf has the highest sublimation rate due to the additional contact conduction contribution, the variation in the sublimation rate between vials 2 (at 6 inches from the door) through vial 5 (9.5 inches away) though prevalent is merely 4.8%. The relative contribution of the top shelf and the Plexiglass door in the heat transfer is evident in the arrangement used in setup 2. The interplay between the roles of the shelf and the glass door in the heat transfer is clearly visible in Figure 10 which summarizes the sublimation rate from each of the vials used in setup 2.

With an increase in the separation distance from the bottom shelf in the continuum limit, the mass flow rate gradually decreases, however, on increasing the separation distance from the bottom shelf beyond the middle of the gap separating the shelves, the effect of the top shelf becomes significant and leads to an increased mass flow rate from the vial. This is attributed predominantly to the radiative and conductive component of the heat transfer from the top shelf and <5% of the heat transfer can be attributed to the contribution from radiation through the door. The difference in the sublimation rates for vial 1 for the two setups may be attributed to difference in performance of the two dryers used for each of the setups. The dryer used for setup 2 may presumably have had a higher chamber-condenser pressure ratio for the same chamber pressure of 100mTorr maintained during the drying cycle. It becomes clear from the results of setup 2 that the separation distances used lead to uncertainty regarding the relative roles of the top and bottom shelves. In order to minimize the involved uncertainty, setup 3 was used. The results from the setup 3 are discussed in the following section.
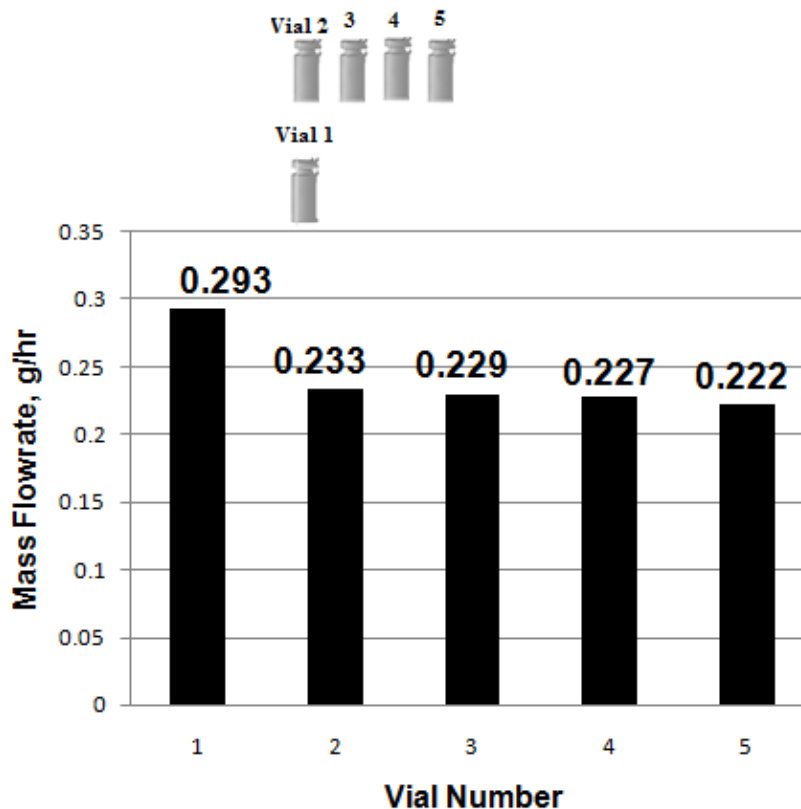
American Institute of Aeronautics and Astronautics

Figure 9. Mass Flow rate of Individual Vials at a chamber pressure of 100mTorr: Setup1

B. Setup 3: Conduction, Convection and Radiation in Primary Drying

The objective of using this setup was a) eliminate the uncertainty caused by the heat transfer from the top shelf b) to suspend multiple vials placed at similar distances from the shelf (1-3mm) as would be used during a typical manufacturing cycle using pre-filled syringes c) to vary the heat transfer between the different flow regimes that were described earlier, to help predict the individual heat transfer contributions. Figure 11 summarizes the measured mass flow rate of the individual vials for a chamber pressure of 100mTorr. The mass flow rate of two vials for each separation is shown. Similar mass flow rate data were obtained for chamber pressures varying between 10-200mTorr and equation 12 was used to obtain the heat flux across the vial surface. The following section discusses the variation in the heat flux across the vials as a function of the chamber pressure.
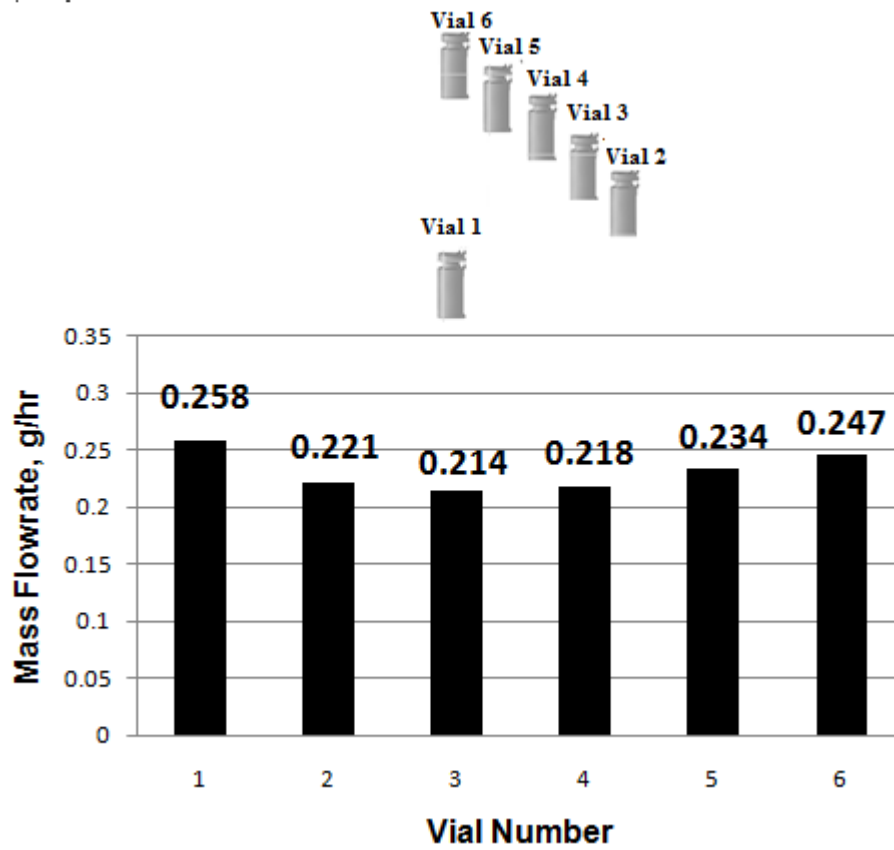
12
American Institute of Aeronautics and Astronautics

Figure 10. Sublimation rates of Individual Vials at a chamber pressure of 100mTorr: Setup2
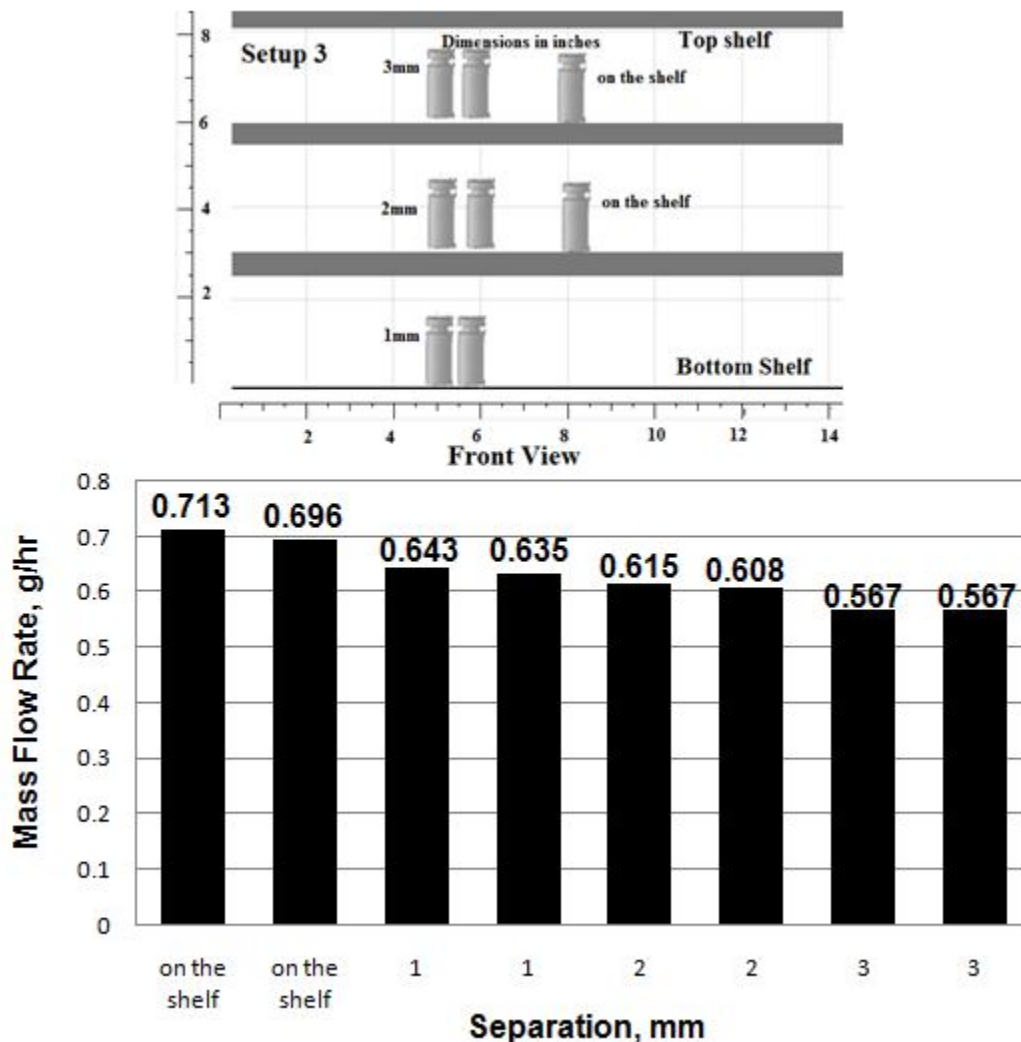
Figure 11. Sublimation rates at a chamber pressure of 100mTorr: Setup3

Among the different heat transfer components that were discussed earlier, the radiative and contact conduction terms alone are independent of pressure. The convective component and the heat transfer that takes place through the gas in the gap separating the vial and the shelf are dependent on pressure in the temperature jump and free molecular regimes. Thus, the y-intercept of the plot of heat transfer as a function of the pressure gives the pressure independent component. At an extrapolated 0 pressure condition (y-intercept), for the suspended vials, the heat flux measured is the heat transfer due to radiation, q_{rad}. And, for the vial on the shelf, at 0 pressure, the heat transfer is the sum of radiative and direct contact contribution. The difference between the 2 intercepts gives the contribution through direct conduction, $q_{contact}$. Figure 12 illustrates the experimentally measured variation in heat flux for different pressures and separation distances. As predicted by the analytical solution described in equation 1, in the free molecular limit, the measured heat flux is found to be independent of the separation. Thus, we see that at a chamber pressure of 10 mTorr where the Knudsen number is greater than 1, the heat flux for all the suspended vials is the same, irrespective of the separation. On increasing the pressure, the heat transfer increases. This increase is attributed to components of the heat transfer that are dependent on pressure i.e. the conduction through the gas in

14
American Institute of Aeronautics and Astronautics

the temperature jump regime and the convective component. The heat transfer through the gas is quantified using the temperature jump equation 5 and the rest of the heat transfer is attributed to the convective heat transfer. The drop in the heat flux for the vial at 2mm separation and a pressure of 200mTorr is presumably due to an error in the experimental measurement.
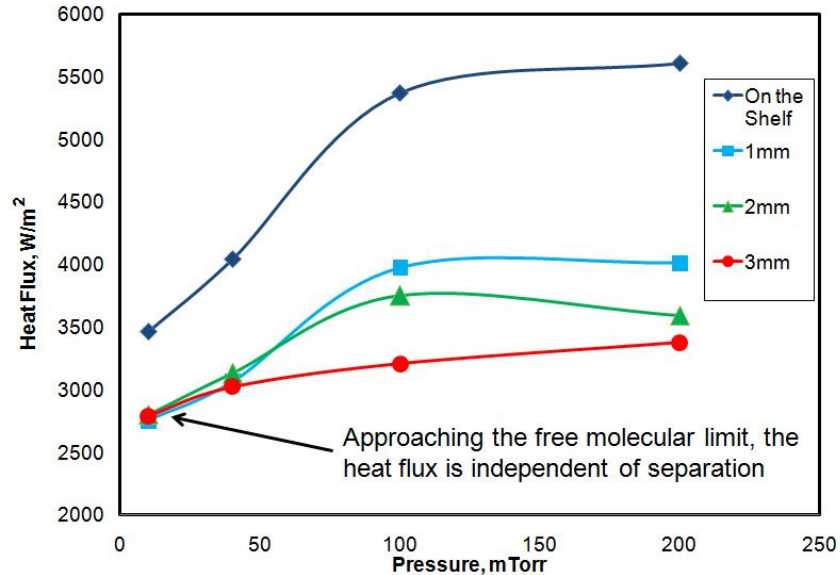

Figure 12. Pressure dependence of Heat Flux for varying separation distances of the vial from the shelf

Figure 13 represents the relationship between the measured heat flux and pressure between 10-100mTorr for each separation with the corresponding y-intercepts. As represented by Eq. (1), the heat transfer in the free molecular limit varies linearly with the pressure. Thus, an equation representing the variation for each separation was used to determine the y-intercept.

The assumptions associated with the calculations for the contributions of the different heat transfer modes are:

1) A hard-sphere water vapor molecular model with a mean water vapor molecular diameter of 5.78˚A was used.

2) The heat transfer through the gas in the gap separating the vial and the shelf assumes 1D heat transfer between parallel plates: This is valid for small separations that we encounter.

3) For the vial placed in direct contact, a nominal separation of 0.4 mm is assumed.

4) For quantifying the heat conduction through the gas, it is assumed that there is no change in the radiative component for the small incremental separations.

5) For quantifying the heat transferred through direct contact, it is assumed that the increase in the heat flux across the vial placed in direct contact juxtaposed with one at a separation of 1mm is only due to contact heat conduction.

6) The error in calculations lies within ±0.4% which is the error in using feeler gauges to measure the separation. Also, testing for repeatability of results at a pressure of 100mTorr for 3 different runs, it was found that the maximum variation in the sublimation rate was within 4%
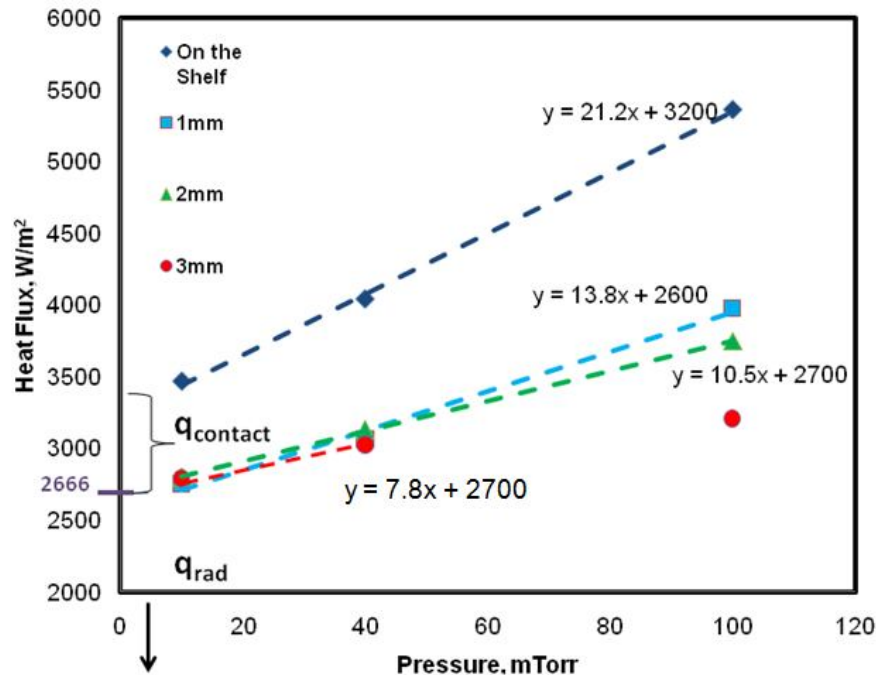
American Institute of Aeronautics and Astronautics

Figure 13. Variation in Heat Flux in the pressure range 10-100 mTorr and the linear expressions representing each of them

Figure 14 illustrates the relative contribution of the different heat transfer modes. While, the contact conduction component contributed 11% to 17% of the total heat transfer for the vial placed on the shelf, the radiative component varied from 47% of the total heat transfer for the vial placed on the shelf to 94 % of the total heat transfer for the vial placed at a separation of 3mm from the shelf for the suspended vials. On increasing the pressure, the heat transfer increases. This increase is attributed to components of the heat transfer that are dependent on pressure i.e. the conduction through the gas in the temperature jump regime and the convective component. The contribution from gas conduction at 200mTorr for the vial placed on the shelf amounts to 21% of the total heat transfer and the corresponding convective component amounts to 20% of the total heat transfer. This reduces to 4.2% and 1.2% respectively at a pressure of 10mTorr and a separation of 3mm. Even though the radiative component is dominant among the heat transfer modes, it has a fourth power dependence on the shelf surface temperature. Hence, the gas conduction and convective components become increasingly important in the heat transfer during a primary drying cycle that involves lower shelf temperatures. Moreover, we see that the convective component of the heat transfer cannot be ignored at higher chamber pressures (>80mTorr). This contradicts conclusions made in the past on the role of convection in freeze-drying [11].
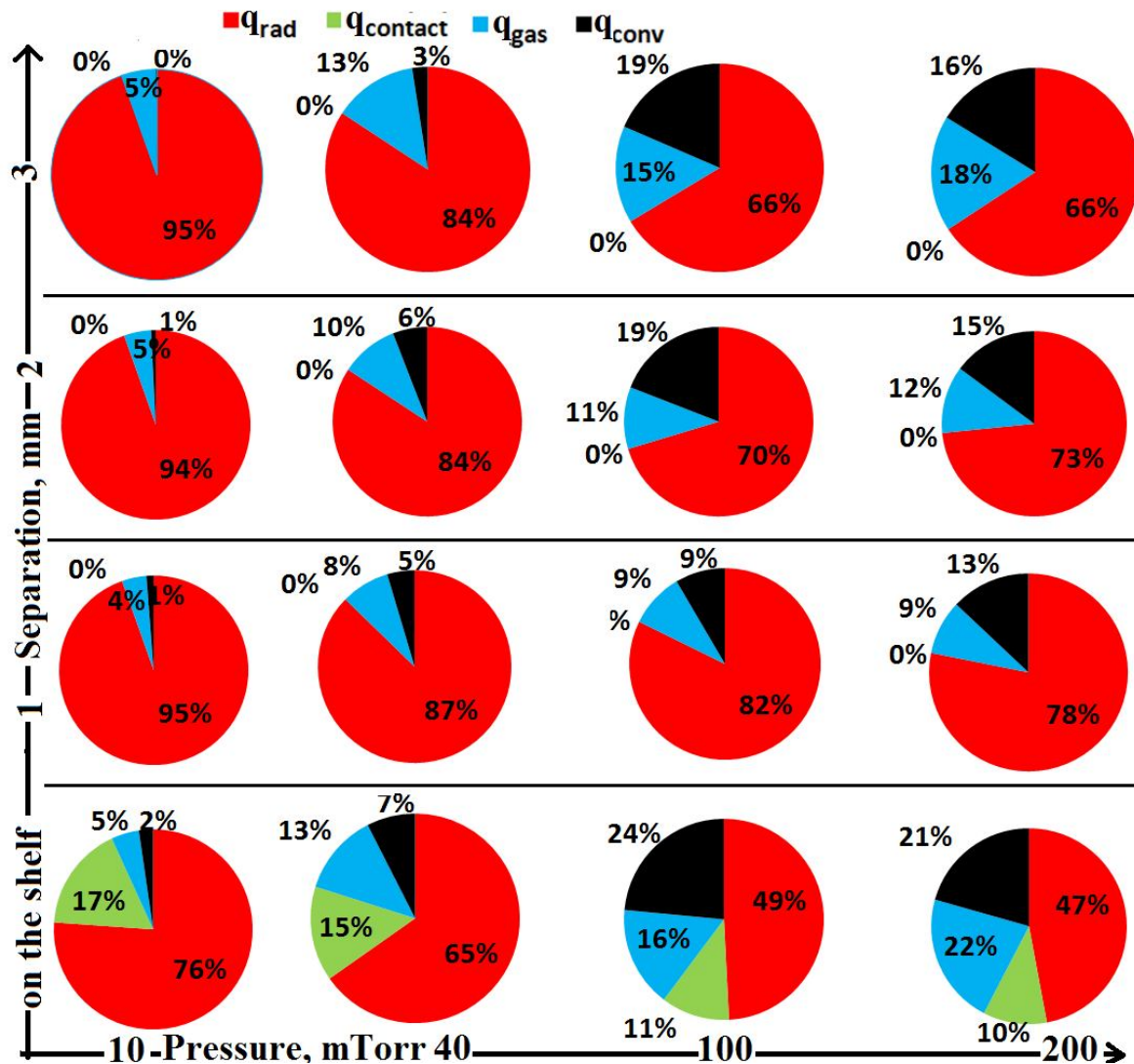
16
American Institute of Aeronautics and Astronautics

Figure 14. Contribution of Conduction, Convection and Radiation in primary drying

V. Conclusions

The current work elaborates on the position dependence of heat transfer in the product chamber and the role played by the different modes of heat transfer during primary drying. The heat transfer studies revealed that the effect of radiation from the glass door in the presence of the radiation shield though small, was not completely eliminated. There was an increase in the drying rate of vials placed close to the glass door. The variation in the sublimation rate between a vial at 6 inches from the door and a vial at 9.5 inches away was merely 4.8%. Apart from radiation effects of the glass door, separation from the shelves plays an important role in determining the sublimation rate of the vials. The vials placed directly on the shelf had the highest sublimation rate which reduced as the separation from the bottom shelf increased. With an increase in the separation distance from the bottom shelf, the mass flow rate gradually reduces up to a level where the top and bottom shelves do not play a significant role through gas conduction. However, on increasing the separation distance from the bottom shelf further, the effect of the top shelf becomes significant and leads to an increased mass flow rate from the vial. This is attributed predominantly to the radiative and conductive component of the heat transfer from the top shelf and <5% of the heat transfer can be attributed to the contribution from radiation through the glass door. The experimental measurements

17
American Institute of Aeronautics and Astronautics

of heat flux across the vial corroborate that the heat transfer in the free molecular limit is independent of separation and hence, at low pressures, the heat flux across the suspended vials was the same in the separation range 1-3mm. The radiative and contact conduction components being independent of pressure, the y intercept of the heat flux-chamber pressure plot was used in identifying their contribution. While contact conduction contributed to 11-17% of the total heat transfer for the vial placed on the shelf, the radiative component varied from 47% of the total heat transfer for the vial placed on the shelf to 94 % of the total heat transfer for the vial placed at a separation of 3mm from the shelf for the suspended vials. On increasing the pressure, the heat transfer increases. This increase is attributed to components of the heat transfer that are dependent on pressure i.e. the conduction through the gas in the temperature jump regime and the convective component. The heat transfer through the gas is quantified using the temperature jump equation and the rest of the heat transfer is attributed to the convective heat transfer. The contribution from gas conduction at 200mTorr for the vial placed on the shelf amounts to 21% of the total heat transfer and the corresponding convective component amounts to 20% of the total heat transfer. This reduces to 4.2% and 1.2% respectively at a pressure of 10mTorr and a separation of 3mm. Thus, the convective component cannot be ignored at higher pressures that are more commonly used in primary drying, something that has traditionally been assumed for suspended vial heat transfer analysis.

Acknowledgments

References

1. S.L. Nail. The effect of chamber pressure on heat transfer in the freeze drying of parenteral solutions. J. Parenteral Drug Assoc., 34, 1980, pp:358–368
2. Pikal MJ, Shah S, Senior D, and Lang JE. Physical chemistry of freeze-drying: measurement of sublimation rates for frozen aqueous solutions by a microbalance technique. J. Pharm. Sci., 72, 1983, pp:635–50
3. M. J. Pikal, M.L. Roy, and S. Shah. Mass and heat transfer in vial freeze-drying of pharmaceuticals: Role of the vial. J. Pharm. Sci., 73, 1984, pp 1224–1237
4. M.J. Pikal. Use of laboratory data in freeze drying process design: Heat and mass transfer coefficients and the computer simulation of freeze drying. J. Parenter. Sci. Technol., 39, 1985, pp 115136
5. S. Rambhatla, S. Tchessalov, and Michael J. Pikal, Heat and Mass Transfer Scale-Up Issues During Freeze-Drying, III: Control and Characterization of Dryer Differences via Operational Qualification Tests, AAPS PharmSciTech, Vol. 7, No. 2, 2006
6. Wei Y. Kuu a; Steven L. Nail a;Lisa M. Hardwick, Determination of Shelf Heat Transfer Coefficients Along the Shelf Flow Path of a Freeze Dryer Using the Shelf Fluid Temperature Perturbation Approach, Pharmaceutical Development and Technology, Vol. 12, Issue 5, 2007 pp. 485 – 494
7. Henning Gieseler and Geoffrey Lee, Effects of Vial Packing Density on Drying Rate during Freeze-drying of Carbohydrates or a Model Protein Measured using a Vial-weighing Technique, Vol. 25, No. 2 , 2008
8. Patel M. Patel, Feroz Jameel and Michael J. Pikal, The effect of dryer load on freeze drying process design, J. Pharm. Sci., Published Online: 10 May 2010
9. Pikal MJ, Cardon S, Bhugra C, Jameel F, Rambhatla S, Mascarenhas WJ, Akay HU, The nonsteady state modeling of freeze drying: in-process product temperature and moisture content mapping and pharmaceutical product quality applications, Pharm Dev Technol. 10(1), 2005, pp. 17-32
10. P. Sheehan, A. I. Liapis, Modeling of the primary and secondary drying stages of the freeze drying of pharmaceutical products in vials: Numerical results obtained from the solution of a dynamic and spatially multi-dimensional lyophilization model for different operational policies, Biotechnology and Bioengineering, Vol. 60 Issue 6, 1998, pp. 712 - 728
11. Shailaja Rambhatla and Michael J. Pikal. Heat and mass transfer scale-up issues during freeze-drying, I: Atypical radiation and the edge vial effect. AAPS PharmSciTech., 4(2): article 14, 2003
12. A. Alexeenko, A. Ganguly, S. Nail, Computational Analysis of Fluid Dynamics in Pharmaceutical Freeze-Drying, Journal of Pharmaceutical Sciences, Vol. 98 (9), , September 2009, pp. 3483-3494
13. S. Dushman and J. M. Lafferty. Scientific Foundations of Vacuum Technique, 2nd ed. Wiley, New York, N.Y. 1962.
14. Bird G.A., Molecular Gas Dynamics and the Direct Simulation of Gas Flows. Oxford Science Publications, 1994
15. Brulls M and Rasmuson A. Heat transfer in vial lyophilization. Int. J. Pharm., 246:1–16, 2002